Journal of Orthopaedics 50 (2024) 49–57

Contents lists available at ScienceDirect

Journal of Orthopaedics

journal homepage: www.elsevier.com/locate/jor

Evaluation of an early-stage prototype polyurethane femoral head implant for hip arthroplasty

Nad Siroros [a,b,c], Ricarda Merfort [a], Filippo Migliorini [a,d,*], Sophie Lecouturier [a], Sophia Leven [a], Maximilian Praster [a], Frank Hildebrand [a], Jörg Eschweiler [e]

[a] Department of Orthopaedics, Trauma and Reconstructive Surgery, University Medical Center RWTH Aachen, Germany
[b] Biomedical Engineering Institute, Chiang Mai University, Thailand
[c] Department of Mechanical Engineering, Faculty of Engineering, Chiang Mai University, Thailand
[d] Department of Orthopaedic and Trauma Surgery, Academic Hospital of Bolzano (SABES-ASDAA), Teaching Hospital of the Paracelsus Medical University, 39100, Bolzano, Italy
[e] Department of Trauma and Reconstructive Surgery, BG Hospital Bergmannstrost, Halle (Saale), Germany

ARTICLE INFO

Keywords:
Bearings
Implant
Hip arthroplasty
Polyurethane

ABSTRACT

Introduction: Thi study evalautes a new bone-preserving femoral head cover that mimics the articular cartilage of the femoral head.

Methods: A specially developed polyurethane (PU) was evaluated in biocompatibility (cytotoxicity test) and mechanical response to tensile loading. In the cytotoxicity test, steam sterilized (SS) and ethylene oxide sterilized (EtO) PU samples were incubated separately in a cell culture medium. The seeded cell line MG-63 was then added to these sample-incubated cell culture mediums. One negative control group and one positive control group were also evaluated. The cells in each group were cultured for seven days before being quantified using the alamarBlue assay. In the mechanical test, the femoral head cover implants were separated into three groups of three samples. Each group represented a different implant insertion idea: direct insertion (*uc* sample) and another two insertion modes (*is* and *ss* samples) representing implants with enclosure mechanisms. The test consisted of distance-controlled cyclic tensile loadings followed by a failure test.

Results: The cytotoxicity test results show no significant difference in fluorescence intensity between the negative control, the three SS groups, and one EtO group ($P > 0.05$). However, the other two EtO groups exhibit significantly lower fluorescence intensity compared with the negative control ($P < 0.05$). In the mechanical test, the *is* samples have the highest cyclic loading force at 559.50 ± 51.41 N, while the *uc* samples exhibit the highest force in the failure test at 632.16 ± 50.55 N. There are no significant differences ($P > 0.05$) among the *uc, is,* and *ss* groups in terms of stiffness.

Conclusion: The cytotoxicity test and the mechanical experiment provide initial assessments of the proposed PU femoral head cover implant. The evaluation outcomes of this study could serve as a foundation for developing more functional design and testing methods, utilizing numerical simulations, and developing animal/clinical trials in the future.

1. Introduction

The hip joint is one of the largest joints in the body. This joint consists of the femoral head sliding within the acetabulum. A strong ligamentous structure and many muscles stabilize the hip joint, making an upright stance and gait possible. Even in normal daily activities, the hip joint bears 2.8–8.7 times the body weight.[1,2] Moreover, during walking, the bending moment and torsion torque in the femoral shaft reach around 3–5% BWm (body weight meter) and up to 3% BWm, respectively.[2,3] Therefore, the articular surface of the hip joint can wear out, and degradation of the local cartilage leads to pain and inflammation, known as osteoarthritis (OA).[4] If non-surgical interventions do not improve the

* Corresponding author. Department of Orthopaedics, Trauma and Reconstructive Surgery, University Medical Center RWTH Aachen, Germany.
E-mail addresses: nsiroros@ukaachen.de (N. Siroros), rmerfort@ukaachen.de (R. Merfort), migliorini.md@gmail.com (F. Migliorini), slecouturier@ukaachen.de (S. Lecouturier), sleven@ukaachen.de (S. Leven), mpraster@ukaachen.de (M. Praster), fhildebrand@ukaachen.de (F. Hildebrand), joerg.eschweiler@bergmannstrost.de (J. Eschweiler).

https://doi.org/10.1016/j.jor.2023.11.067
Received 22 November 2023; Accepted 26 November 2023
Available online 29 November 2023

patient's quality of life, the next step is hip arthroplasty.[5] At present, more than 1 million interventions are performed annually worldwide.[6] In 2021, Germany documented over 230,000 hip arthroplasty cases and over 32,000 revision, change, or removal cases.[7] There are two possible surgical procedures for patients with end-stage degenerative hip conditions: total hip arthroplasty (THA) and hip resurfacing arthroplasty (HRA).[8]

THA and HRA have become popular treatments for OA patients and achieve satisfactory outcomes, with no significant difference in the revision rates of THA and HRA.[9] However, one disadvantage of THA is the loss of natural bone, which could lead to complications, especially in the case of revision surgery. For HRA, the femoral head is capped, and the bone of the proximal femur is preserved.[10] This is an advantage over THA in terms of bone preservation. It is preferable, especially in younger patients and active patients,[11] to preserve the femoral head and avoid the implantation of intramedullary devices required in THA. Another advantage of HRA is the reduced risk of dislocation associated with the use of large femoral heads.[12] The two main reasons for revision in HRA are femoral neck fractures[11,13] and cup malposition[11]; THA largely eliminates the risk of femoral neck fractures. However, it is evident that both THA and HRA provide patients with approximately 15–25 years[14] before a new implant is required. As issues such as large bone loss due to intramedullary implant and femoral neck fractures occur in the femur, this research focuses on the femoral head, rather than the acetabulum.

Currently, a number of materials are used for hip arthroplasty. The femoral head is usually metal or ceramic, while the acetabulum can be either metal, ceramic, or a polymer.[15] Besides conventional hip joint bearings, there have been studies on "compliant bearings" that mimic the mechanical properties of the articular cartilage (low modulus and the capability of large deformation without failure).[15–17] These so-called "cushion bearings" are polyurethane (PU), mainly with a polycarbonate-urethane (PCU) acetabulum cup component. This material has a lower wear rate and lower friction compared with polyethylene.[16] Other reasons to consider PU over PE are its greater heat stability, hydrophilicity, and lower cytokine response and osteolysis produced by wear debris.[16,18] To date, THA and HRA interventions have been performed using hip joints with ceramic or metal femoral heads on PCU acetabular components (Merola and Affatato, 2019), but not with PU as the femoral head component. This motivated us to examine the conceptual idea of a naturally soft femoral head implant mimicking the human articular cartilage, enabling bone and soft-tissue preservation without increasing surgical complexity. As a result, in collaboration with revomotion GmbH Cologne and Fraunhofer UMSICHT, the first iteration of the femoral head implant was proposed in the form of a soft-material femoral head cover (Fig. 1) made of a specially developed PU.

As for all medical devices and prostheses implanted in connective tissue immediately induce an initial host response to act against the foreign body,[19] the implant should be biocompatible with the body even after being sterilized. Futhermore, new implant design functional assessment can be performed numerically and experimentally according to the objectives of the test. The determination of appropriate experimental load cases and joint ambientes, as well as testing apparatus, is essential in the current development stage of this research.

Therefore, in the early-stage development of this study, the first objective is to preliminarily assess implant biocompatibility using cytotoxicity test. The second objective is to investigate the femoral head cover response to tensile loading and the initial implementation concept. The preliminary assessment is intended to provide information for further development. It is hypothesized that the PU material is not toxic to human cells, and the mechanical test results should provide an overview of how each implantation approach responds under a given loading condition.

2. Materials and methods

This section describes the materials and methods applied for biocompatibility and mechanical testing. Two different forms of specially developed PU samples were evaluated: in punch form for biocompatibility testing and in implant form for the mechanical tests (Fig. 2). All samples were provided by revomotion GmbH, Cologne, Germany. An overview of the biocompatibility and mechanical tests can be found in Appendix A.

2.1. Materials and methods for the biocompatibility test

The PU samples measured 6 mm in diameter and 4 mm in height, as

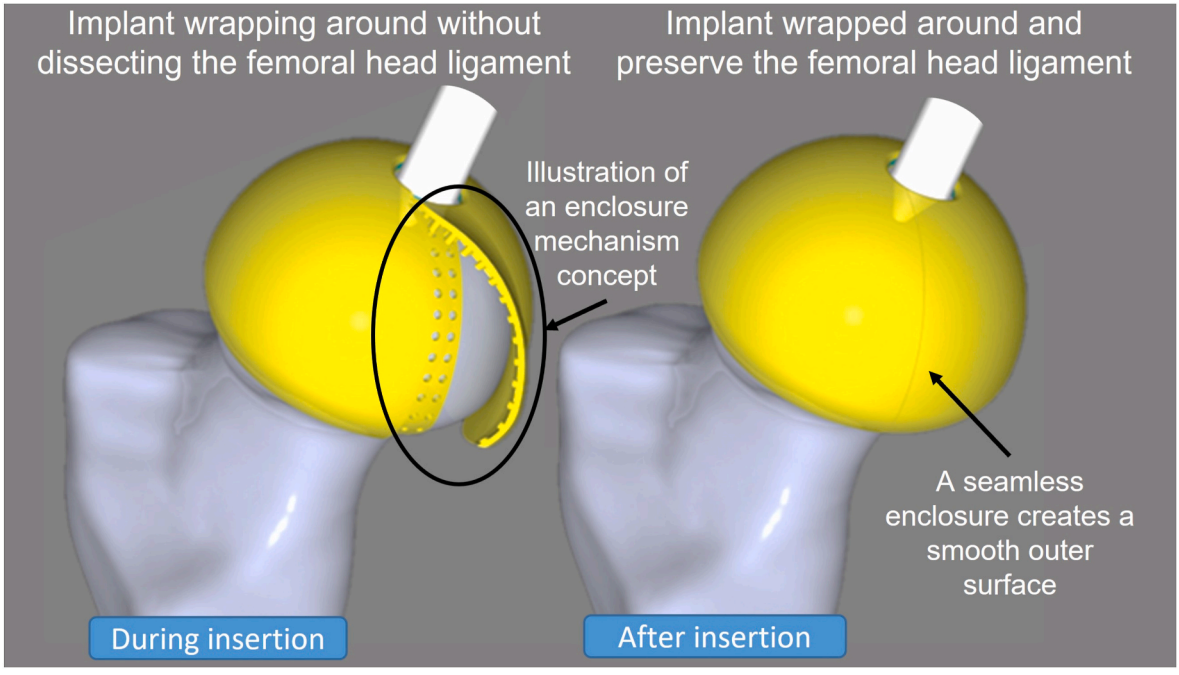

Fig. 1. Conceptual design of a femoral head implant during insertion (left) and wrapped around (right) the femoral head, preserving bone and femoral head ligament.

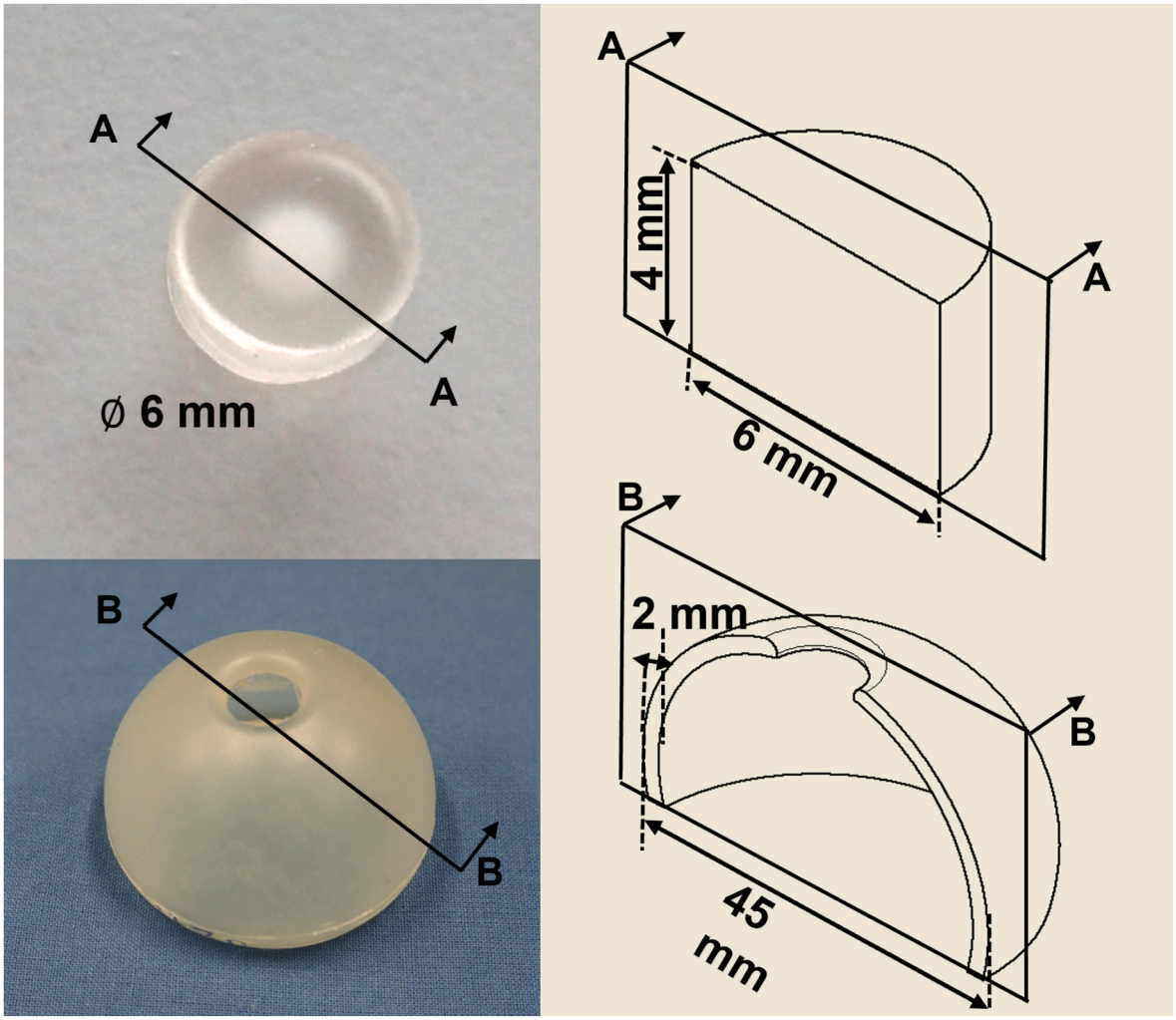

Fig. 2. Geometry of the PU sample for biocompatibility test (top) and mechanical test (bottom).

shown in Fig. 2 (top). The samples were delivered in six groups of five small punches (30 samples in total). Three sample groups were sterilized with steam (autoclave) (SS) and the other three sample groups were sterilized with ethylene oxide (EtO) according to the sterilization of healthcare products standards for autoclave and EtO (ISO 17665 and ISO 11135), respectively.[20]

Cell line MG-63 (ECACC 86051601, Sigma-Aldrich/Merck KGaA, Darmstadt, Germany) was selected for cell cultivation. The cell line is human osteoblast-like osteosarcoma cells, which is commonly used to investigate the cell response to the implant material (i.e., biocompatibility).[21,22] The cell culture medium consisted of DMEM low glucose (Gibco/Thermo Fisher Scientific Inc., Massachusetts, USA), 1% Pen Strep (Sigma-Aldrich/Merck KGaA, Darmstadt, Germany), and 5% FCS (PAN-Biotech GmbH, Aidenbach, Germany). Cells were cultured in an incubator (Binder GmbH, Tuttlingen, Germany) at 37 °C. The reducing environment of the cells was quantified using alamarBlue (Thermo Fisher Scientific Inc., Massachusetts, USA) according to the manufacturer's instructions. The alamarBlue emission and excitation wavelengths were measured at 590 nm and 544 nm, respectively. An evaluation of cell viability was performed by observing the fluorescence intensity using the Optima reader (BMG Labtech GmbH, Ortenberg, Germany).

In preparation for the biocompatibility tests, each sample group was individually incubated in the cell culture medium at 37 °C for one week in a six-well plate (Thermo Fisher Scientific Inc., Massachusetts, USA) to create the sample-incubated cell culture medium. In addition, positive and negative controls were made to provide a reference for cell cytotoxicity evaluation. The negative control was a normal-non-contaminated cell culture medium. In contrast, for the positive control, 60 μg/ml digitonin (Promega Corporation, Wisconsin, USA) was added to the normal-non-contaminated cell culture medium to create a cytotoxic environment.

The test began by seeding the cells in 96-well plates with a density of 1,000 cells per well (Day 0). Using quadruple preparation, four wells were employed for each control and each test group (n = 4). Twenty-four hours after seeding the cells, the first measurement was performed (denoted as time t_0), followed by the first cell culture medium change. For all test groups, the cell culture medium was replaced by the corresponding sample-incubated cell culture medium. For the controls, the cell culture medium was replaced by a normal cell culture medium. Digitonin was added to the cell culture medium wells to create a positive control. Further measurements were performed on Day 2 (t_1), Day 4 (t_2), and Day 7 (t_3). The second cell culture medium change occurred on Day 4. The fluorescence intensity measurements were executed in duplicates and measured with the Optima reader. For this process, the alamarBlue reagent was diluted at a ratio of 1:10 with the cell culture medium and incubated with the cells for 2.5 h at 37 °C. The fluorescence intensity results of each measurement were recorded.

2.2. Materials and methods for the mechanical test

Nine prototypes of PU femoral head cover implant were produced,

each measuring 45 mm in diameter with a shell thickness of 2 mm. The concept of the femoral head implant is to preserve bone and soft tissue; consequently, two insertion approaches were considered in the mechanical test procedure: direct insertion and "femoral head wrapping-around" insertion to preserve the femoral head ligament (ligamentum teres femoris).

For the direct insertion, the samples remain uncut (*uc* samples). This mode served as a reference in the tests. For the wrapping-around insertion, the samples must be cut longitudinally (vertically) and enclosed. For this instance, two enclosure (locking) mechanisms ideas were introduced: 1) the "point-to-point" enclosure, whereby the cut is held perpendicular to the cut line, and 2) the "continuously running" enclosure, in which the cut is continuously held at an angle along the cut line. To represent the enclosure function mechanisms, the cut samples were sutured with surgical suture material (Prolene Polypropylene, MPP7756, Ethicon, Ohio, USA) using two different suture techniques: a simple interrupted suture (*is* samples) and a running subcutaneous suture (*ss* samples), as shown in Fig. 3(b) and (c), respectively. Hence, in the preparation stage, the samples were divided into three groups (*uc, is, ss*), each consisting of three samples.

The test setup idealized tensile forces through the implant as it created an extreme worst-case scenario for the enclosure mechanisms. The implant was placed on a 3D-printed femoral head separated in the middle. The half-femoral head parts were 3D printed (Ultimaker B.V., Ultrecht, Netherlands) to fit the inner diameter of the implant. The c-arm parts were connected to a 10-kN tensile testing machine (ZwickRoell, Ulm, Germany), as shown in Fig. 3. The c-arm parts were designed to keep the mass center of the artificial femoral head in line with the tensile force, thus minimizing the moment during the test. To date, there is no specific test standard for these PU implants and their containment mechanisms. Therefore, the test protocol was designed to perform three cyclic loads at a rate of 30 mm/min up to a maximum displacement of 20 mm followed by a pull-to-failure test (or up to the set maximum displacement of 50 mm). The cyclic procedure was chosen to investigate the overall response of each implant setup to the given mechanical loads. The maximum force during each cycle and at failure was measured. The maximum displacement of 20 mm for the cyclic test and 50 mm for the failure test was set to allow clear visual observation of each implant setup. The testing machine recorded the force and the displacement. The experimental footage was also recorded for visual observation.

2.3. Statistics

Statistical analyses were applied to the results of both the biocompatibility and biomechanical testing. The mean and standard deviation were calculated for the biocompatibility tests, and selected parameters were analyzed using a two-tailed *t*-test, with statistical significance indicated by P-values of less than 0.05. In addition, the gradients of the load–displacement curves were analyzed descriptively using the R-squared value.

3. Results

3.1. Biocompatibility testing

This section presents the results of the SS and EtO sterilization groups and compares them with the positive and negative controls. The cell reduction during the alamarBlue assay results in fluorescence intensity changes. Fig. 4 shows the average fluorescence intensity measurement value of the positive control, negative control, and every sample-incubated cell culture medium group at four measurement time periods (t_0, t_1, t_2, and t_3). The higher fluorescence intensity indicates higher viable cells. The fluorescence intensity results of the positive and negative controls represent cell toxicity and non-toxicity references, respectively. The measurement results of all sample-incubated cell culture medium groups exhibit a similar trend to the negative control. The fluorescence intensity measurements at times t_1 and t_2 indicate that all sample-incubated cell culture medium groups have lower fluorescence intensity than the negative control. At time t_3 (Day 7), the fluorescence intensity of the cell culture medium from all three SSs has no significant difference from the negative control ($P = 0.5$, $P = 0.8$, and $P = 1.0$ for SS 1, SS 2, and SS 3, respectively). In contrast, although the fluorescence intensity in all EtO samples exhibit similar trends to the negative control, only the cell medium culture from EtO 1 shows no significant difference ($P = 0.1$) on the last measurement, while EtO 2 and EtO 3 give significantly lower values ($P < 0.05$) than the negative control. The table showing the fluorescence intensity measurement on the last day can be found in Appendix B.

3.2. Mechanical testing

First, during the first test of the *ss* sample, the suture ruptured at 8

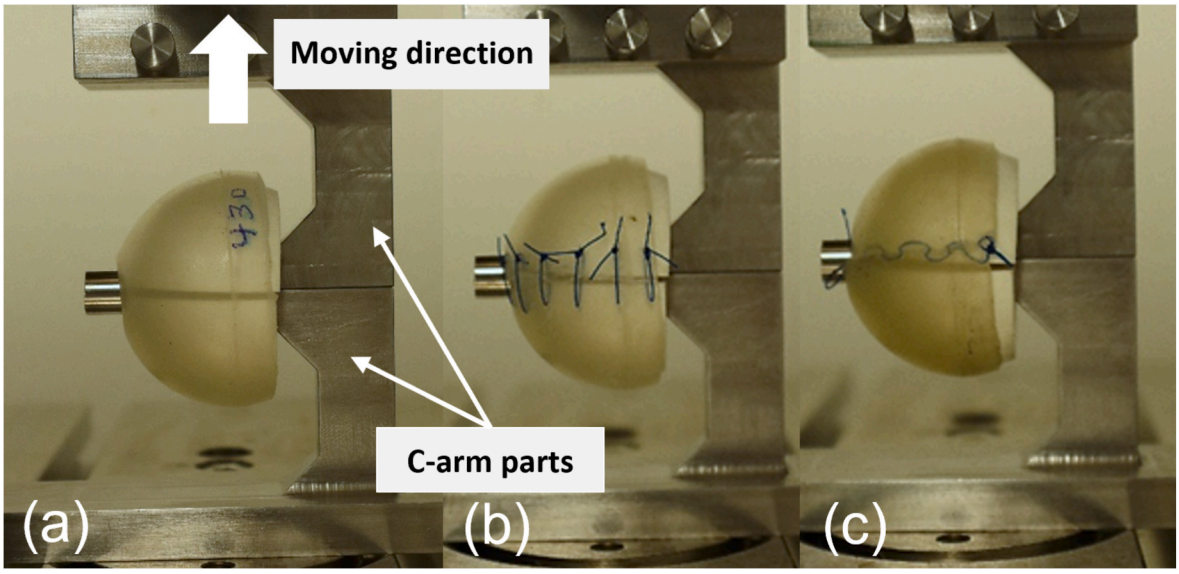

Fig. 3. Experimental setup with upper and lower c-arm parts, which pull the femoral head apart. The three femoral head cover setups are (a) uncut/without suture (*uc*), (b) with simple interrupted suture (*is*), and (c) with running subcutaneous suture (*ss*).

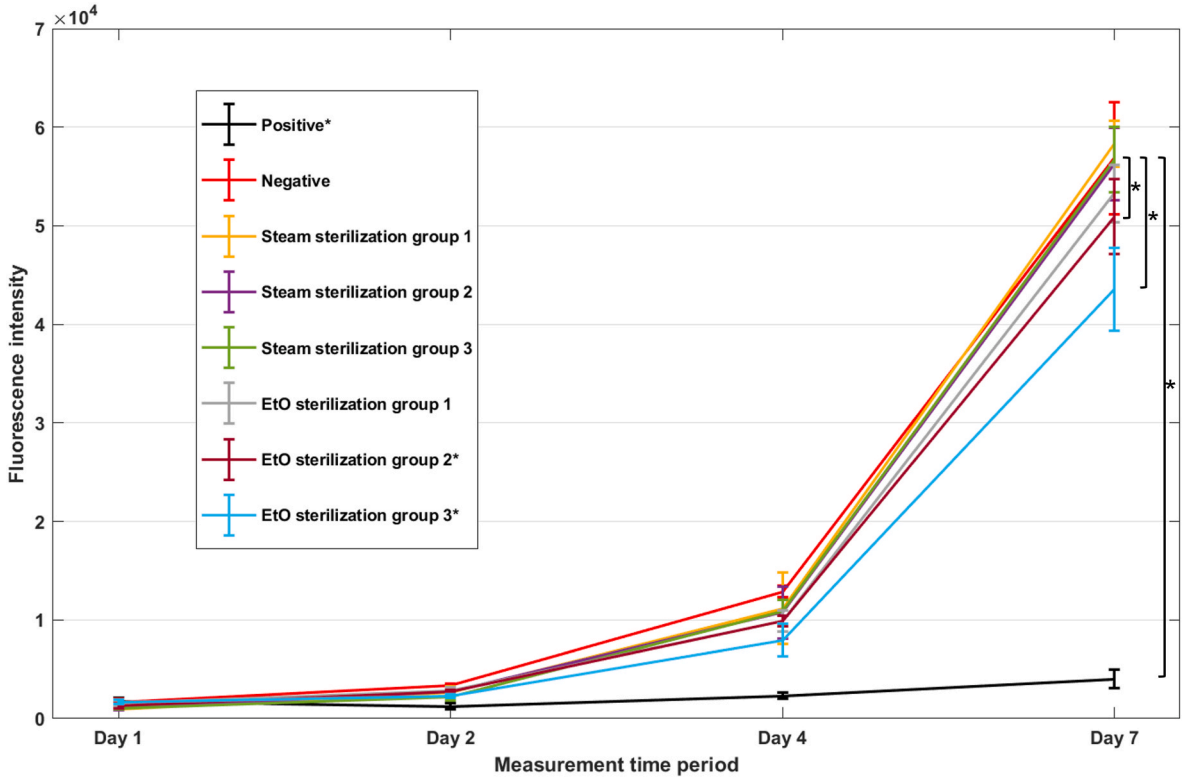

Fig. 4. AlamarBlue assay results of each group on Day 1, Day 2, Day 4, and Day 7 (* P > 0.05 in comparison to the negative control on Day 7).

mm. Therefore, for the *ss* test setup, the maximum displacement was changed from 20 mm to 5 mm. After all tests, all three *uc* samples (n = 3), two *is* samples (n = 2), and two *ss* samples (n = 2) survived. One *is* sample failed during the third cycle. Table 1 presents the average maximum force during the cyclic test, the average maximum force in the failure test, and the stiffness of the first linear part of each cycle. The *is* samples exhibit the highest average maximum force during the cyclic test, followed by the *uc* samples and *ss* samples. The maximum force during the cyclic test for the *uc* samples is nearly three times more than that of the *ss* samples. In the failure test, two *is* samples reached the set maximum limit of 50 mm without failure. Therefore, the maximum force was recorded at this point. At failure, the *uc* sample was subjected to approximately twice the maximum force of the *ss* sample. The stiffness can be determined by the first linear region of each sample. On account of the small tolerance of the experimental setup, the result at the initial position should be ignored. The starting point of the curve begins at 0.4 mm, except for the second cycle of the first *uc* sample, which begins at 1.6 mm. The average R-squared value of all curves is 0.991 ± 0.002. The *uc, is*, and *ss* samples fit approximately 8% (1.6 mm), 5% (1.0 mm), and 45% (2.2 mm) of the displacement, respectively. The *uc* samples exhibit the best stiffness, followed by the *is* samples and *ss* samples. In addition, there is no significant difference when comparing the stiffness of each group (P = 0.6, P = 0.2, P = 0.2 for *uc-is, uc-ss,* and *is-ss*, respectively).

Table 1
Average maximum force during cyclic test, average maximum force in failure test, and stiffness of the first linear part in each cycle.

Sample	Maximum cyclic loading force (N)	Maximum force at failure (N)	Stiffness (N/mm)
uc (n = 3)	433.9 ± 22.7	632.2 ± 50.6	34.6 ± 10.3
is (n = 2)	559.5 ± 51.4	596.3 ± 19.3	30.8 ± 19.5
ss (n = 2)	151.7 ± 48.6	306.9 ± 67.2	27.9 ± 5.4

**uc* = uncut sample, *is* = simple interrupted suture sample, *ss* = running subcutaneous suture sample.

Besides the overall assessment results in Table 1, the behavior of each sample setup can be further investigated. Fig. 5 shows the force–displacement diagram as a representation of the *uc*, *is*, and *ss* samples. Different colors represent each cycle, from the first (blue), second (green), and the last (orange) cycle. A visual observation indicates that the *uc* and *is* samples require less force to produce the same displacement after the first cycle. With the *is* samples, the force needed for the same displacement becomes even lower in the third cycle. However, for the *ss* samples, the trend cannot be determined.

Furthermore, Fig. 5(a) and (b) show that the stiffness decreases toward the third cycle for the *uc* and *is* samples ($k_{uc}^1 = 42.8$N/mm; $k_{uc}^2 = 40.7$N/mm; $k_{uc}^3 = 28.7$N/mm, and $k_{is}^1 = 54.9$N/mm; $k_{is}^2 = 28.8$N/mm; $k_{is}^3 = 22.0$N/mm). For the *ss* sample, Fig. 5(c) indicates that the stiffness values are within 1 N/mm of each other ($k_{ss}^1 = 23.4$N/mm; $k_{ss}^2 = 24.2$N/mm; $k_{ss}^3 = 23.8$N/mm).

Finally, Fig. 6 shows an example of the maximum load at failure of the *uc*, *is*, and *ss* samples. The uncut structure is able to dissipate the force, even with a displacement of 50 mm. In contrast, the two sutured structures suffer a sudden rupture at displacements of 27 mm (*is* sample) and 17 mm (*ss* sample).

4. Discussion

This paper has introduced a new alternative for hip arthrosis treatment to overcome the limitations of THA and HRA. The conceptual ideal of minimizing bone loss and tissue preservation while mimicking the articular cartilage of the femoral head. This idea created an additional arthroplasty option without irreversibly destroying the bone, which could serve 1) younger patients, for whom it is important to increase the time before HRA and/or THA is required, and 2) older patients, for whom reducing the risks and possible complications of THA and HRA is vital.

As the development idea is to replace the articular cartilage, the geometry of the femoral head cover implant with a 45-mm diameter and

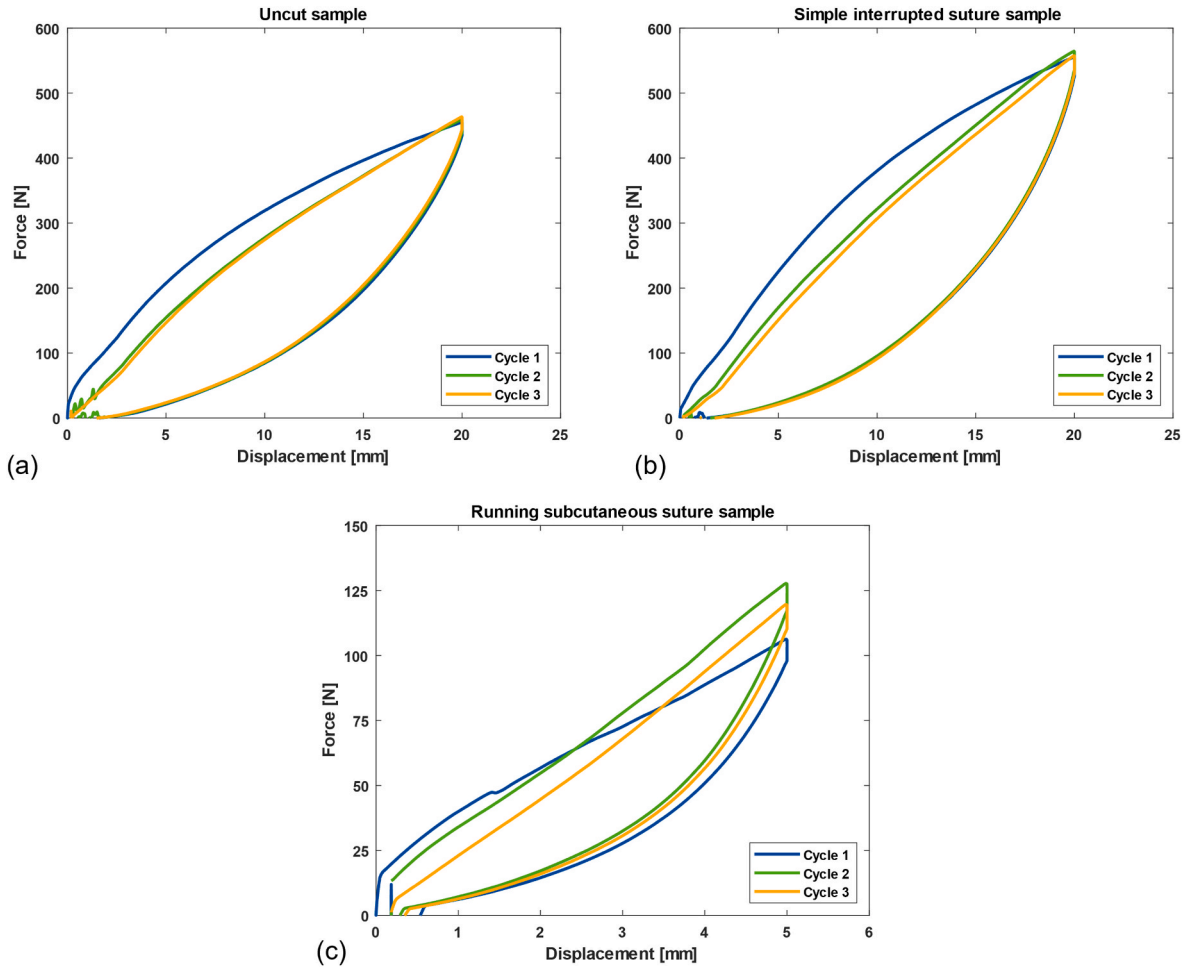

Fig. 5. Left: Force-displacement diagram of femoral head cover (a) uncut/without suture (*uc*), (b) with simple interrupted suture (*is*), and (c) with running subcutaneous suture (*ss*).

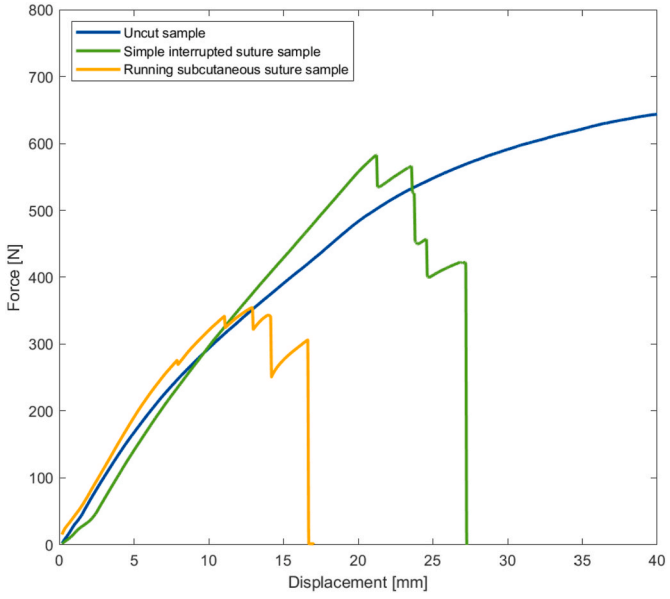

Fig. 6. Example of load to failure curve comparing the three different implants.

2-mm thickness is congruent to the natural size of the femoral head from 40 to 55 mm,[23,24] and a mean cartilage thickness ranging from 1.35 to 3.40 mm.[25–27] This arguably provides more stability, a wider impingement-free movement range, and decreased risk of dislocation due to its larger diameter compared with the typical 32–36 mm femoral head size in THA.[23] In addition, the PU implant prototypes had a compliant bearing, also called a cushion bearing, providing large deformation capability without failure.[15,16] It offer a theoretical reduction in wear and lower friction due to its flexibility and hydrophilic properties.[16] Because the joint size varies among patients, a patient-specific approach (i.e., in manufacturing or intervention workflow) should be initiated. And also the testing methods of the bearing system should be determined to validate the theories underlying PU implants and optimize the hip joint design.

The cytotoxicity tests were performed to determine the biological response to the material[28] using alamarBlue bioassay. The assay is non-radioactive, simple, non-labor intensive, low cost, non-toxic, and enables rapid assessment[29,30] and has been used in tests across a wide range of cell types including in medical research involving human and animal cells.[31] MG-63 is a commonly used osteoblastic model in studies of bone cell viability, adhesion, and proliferation on the surfaces of load-bearing biomaterials.[32] SS (autoclaving) and EtO sterilization, which are common medical device and implant sterilization methods,[33,34] were used to sterilize the PU samples. The cytotoxicity of the samples sterilized by these two methods was then compared.

After sterilization, each group of PU punches was incubated separately in a culture well (using a six-well plate) for one week to transfer

potential cytotoxic contaminants from the sample group to the cell culture medium. This is to promote consistency of cell attachment and proliferation and to minimize errors in medium change and fluorescence intensity measurement. Negative and positive controls set non-cytotoxic and cytotoxic references against which the test groups could be measured. In the positive control, digitonin prevented proper proliferation, in opposition to the negative control. The trends of the fluorescence intensity measurements indicate the non-cytotoxicity, implying that the PU material released no cytotoxic contaminant after sterilization. The measurement results at t_3 show the consistency of the SS group, indicating good sterilization options for the implants. Despite EtO sterilization being the most efficient method for polymeric and soft medical devices,[34] factors such as EtO residual content could influence cell cultivation. In this early-stage development, it is still not possible to determine the effect this implant will induce in the immune system. Following this initial assessment of the biocompatibility of the implant material, further work toward the development of the implant, and further *in-vivo* testing models must be carried out.

The objective of the mechanical testing was to observe the behavior of the three implant implementation ideas. The mechanical response of each setup did not represent the material behavior of the PU material, but the response of the setup to tensile loading. The tensile loading was intended to provide an extreme load to the enclosure mechanism. The cut and the suture techniques were not intended to be used in actual operations, but simply to represent the idea of possible implant enclosure design. From the average maximum force during the cyclic tests and the average maximum force to failure of the *uc, is,* and *ss* samples, the *ss* samples were found to be the least stable. Compared with the *uc* sample, the maximum load reached only about one-third in the cyclic loading and about half in the failure test, and the *ss* samples produced less consistent outcomes than the *uc* and *is* samples when considering the standard deviation. The insertion of the *is* samples led to an increase in load resistance compared with the benchmark. This is mainly due to the stronger material behavior of the inserted threads, which produces an overall stronger structure. In addition, the load resistance results of the two enclosure mechanisms were to be expected, as the *ss* samples consisted of a single suture running along the cut while the *is* samples included six sutures. The failure of the *is* and *ss* samples occurred at the suture in all cases. This means that the PU material is strong enough at this load range. The visual observations during the test indicate that the load is distributed along the cut by the suture due to the nature of running subcutaneous sutures (run along the cut). The simple interrupted suture was considered as another enclosure approach, where the suture runs axially to the load direction. This caused the load to be distributed through the suture hold on both sides of the cut. From these results, the *ss* enclosure mechanism is better under the condition that the enclosure material is strong enough. In the case that the enclosure cannot withstand the load, the *is* enclosure may be more suitable.

In the first linear region of each cycle, there was no significant difference between the stiffness of each setup. At the beginning of the curve, at approximately 1–2 mm, all setups performed similarly. However, when looking further at individual cycles, the stiffness changes as a result of changes in the mechanical properties of each setup. This reflects the influence of the enclosure mechanisms and materials compared with the reference. From this finding, the stiffness parameter is not the major influencing parameter for the development of the enclosure system. Therefore, the influence parameters can be based on the suitable function of the enclosure system design and its material properties, as stated in the previous paragraph. Furthermore, regarding the implementation, it is necessary to define whether the femoral head ligament should be preserved. If the femoral head ligament is to be preserved, the suturing technique will affect the development of the enclosure mechanism. The future development of enclosure mechanisms should provide a smooth outer surface of the femoral head cover and withstand multi-directional loading from any related activities.

Considering that this study covers the early stage of development, there are limitations and improvements to many aspects of the experiments. First, the cytotoxicity tests measured the fluorescence intensity, but did not count the number of cells. Even though this was sufficient to determine biocompatibility, the cell count could enhance the evaluation of the results. Second, the prototype was initially focused on the specially developed PU mixture as material punches, and relatively few femoral head implants were manufactured. Therefore, a higher number of samples could improve the statistical outcomes. Third, concerning experimental tolerance and error, the sample cutting and suturing, and the inconsistent initial position of the force–displacement curve, could be improved. Regarding the inconsistency of the initial position during each cycle, this was due to the fitting of the implant to the experimental femoral head components. Lastly, a numerical simulations were not performed due to limitation of several unknow conditions such as material's properties, material's behaviour (nonlinear expression), and multi-material condition. In the future, simulations can be applied many aspects, such as optimizing the hip joint in terms of geometrical design, surface design for joint lubrication,[35] and the wear and loading of the implants/joint in various conditions.[15,36,37]

Finally, as an outlook for the improvement of implant design and testing, further design improvements are suggested concerning the inner surface design (femoral head–implant interaction), the outer surface design (acetabular–implant interaction), and the investigation of mechanical properties of the material. For the inner surface design, the interaction of the inner surface with the femoral head surface should be determined, e.g., a porous structure for bone ingrowth or a cement fixation as well as the surgical procedure. For the outer surface design, the outer surface should mimic the low friction and smooth surface of the articular cartilage. As an alternative, a dimpled pattern could be applied to the surface to reduce friction.[38] However, the outer surface has to be considered alongside the interaction with acetabular components and should optimize the wear performance.[39] The enclosure mechanism should offer a seamless design to ensure a smooth outer surface. In terms of mechanical properties, the PU material properties must be clearly determined, including mechanical investigations of the wear pattern and high-cycle assessments of the synovial joint environment.

5. Conclusion

In summary, a novel prototype for hip arthroplasty was presented as part of this paper. The positive test results regarding biocompatibility show that insertion into the human body is possible. The development of an insertion method was also shown to be satisfactory in the mechanical tests. In the next step, more specific biocompatibility tests will be conducted to examine the steam and EtO reaction to the material, longer-term cell cultivation, compatibility tests in various environments, and possibly animal trials in the distant future. Furthermore, this evaluation of an early-stage prototype PU femoral head implant has provided initial impressions of the developed implant in terms of both preliminary biocompatibility and mechanical tests. The results obtained in this study are beneficial for the development of implants that, hopefully, will contribute to hip arthrosis treatment in the foreseeable future.

Data availability statement

The original contributions presented in the study are included in the article; further inquiries should be directed to the corresponding author.

Use of AI tools

The authors declare that no AI tools has been used.

Ethical statement

This research did not involve live animals or human subjects; ethical

approval is not applicable.

Funding

The research was funded by "Europäischen Fonds für regionale Entwicklung (EFRE)" and from North Rhine Westphalia (MioHip; EFRE-0800393).

CRediT authorship contribution statement

Nad Siroros: Conceptualization, Formal analysis, Investigation, Methodology, Resources, Visualization, Writing – original draft. **Ricarda Merfort:** Writing – review & editing. **Filippo Migliorini:** Writing – review & editing. **Sophie Lecouturier:** Data curation, Formal analysis, Investigation, Methodology, Writing – original draft. **Sophia Leven:** Methodology. **Maximilian Praster:** Writing – review & editing. **Frank Hildebrand:** Supervision. **Jörg Eschweiler:** Conceptualization, Funding acquisition, Project administration, Resources, Software, Supervision, Writing – review & editing.

Declaration of competing interest

The authors declare that the research was conducted in the absence of any commercial or financial relationships that could be construed as a potential conflict of interest.

Acknowledgments

The authors would like to thank the team members, Dr. Yu Liu, Dr. Luis Fernando Nicolini and Marx Ribeiro, as well as two student assistants, Ramon Sirilertworakul and Kuang-Cheng Yang, for assisting in this study. The authors also wish to thank the project partners, revomotion GmbH Cologne and Fraunhofer UMSICHT, for their assistance during this collaboration.

Appendix A. Preparation overview of biocompatibility and mechanical test

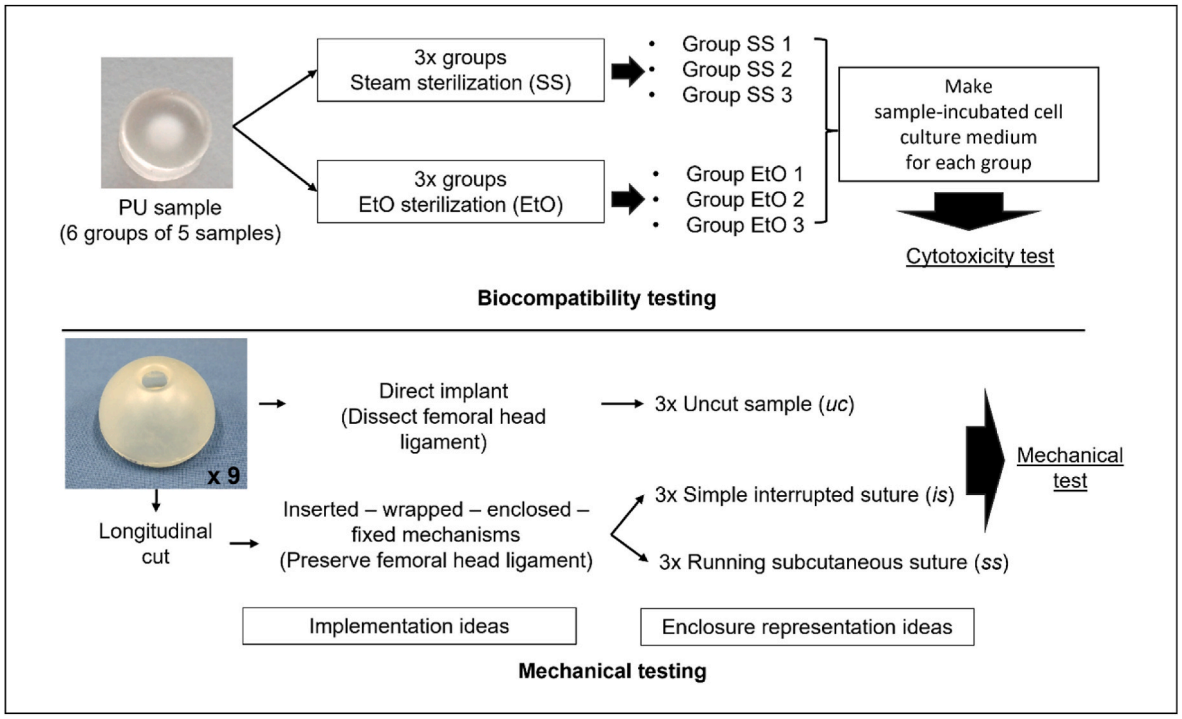

Appendix B. Day 7 (t_3) results of all sample groups compared with the negative control

Group	Fluorescence intensity measurement	P-value
Negative control	56,848 ± 5,685	–
Steam Sterilization Group 1	58,305 ± 2,299	0.5
Steam Sterilization Group 2	56,229 ± 3,661	0.8
Steam Sterilization Group 3	56,717 ± 3,305	1.0
EtO Sterilization Group 1	53,263 ± 2,883	0.1
EtO Sterilization Group 2	50,923 ± 3,837	<0.05
EtO Sterilization Group 3	43,553 ± 4,190	<0.05

References

1. Bergmann G, Graichen F, Rohlmann A. Hip joint loading during walking and running, measured in two patients. *J Biomech*. 1993;26(8):969–990. https://doi.org/10.1016/0021-9290(93)90058-M.
2. Palmowski Y, Popović S, Kosack D, Damm P. Analysis of hip joint loading during walking with different shoe types using instrumented total hip prostheses. *Sci Rep*. 2021;11(1), 10073. https://doi.org/10.1038/s41598-021-89611-8.
3. Haffer H, Popovic S, Martin F, Hardt S, Winkler T, Damm P. In vivo loading on the hip joint in patients with total hip replacement performing gymnastics and aerobics exercises. *Sci Rep*. 2021;11(1), 13395. https://doi.org/10.1038/s41598-021-92788-7.
4. Felson DT. Epidemiology of hip and knee osteoarthritis. *Epidemiol Rev*. 1988;10(1):1–28. https://doi.org/10.1093/oxfordjournals.epirev.a036019.
5. Pivec R, Johnson AJ, Mears SC, Mont MA. Hip arthroplasty. *Lancet*. 2012;380(9855):1768–1777. https://doi.org/10.1016/S0140-6736(12)60607-2.
6. Singh JA. Epidemiology of knee and hip arthroplasty: a systematic review. *Open Orthop J*. 2011;5:80–85. https://doi.org/10.2174/1874325001105010080.
7. Bundesamt Statistisches. DRG-Statistik 2021 - vollstationäre Patientinnen und Patienten in Krankenhäusern Operationen und Prozeduren (OPS Version 2021). https://www.destatis.de/DE/Themen/Gesellschaft-Umwelt/Gesundheit/Krankenhaeuser/Publikationen/Downloads-Krankenhaeuser/operationen-prozeduren-5231401217014.pdf?_blob=publicationFile. Accessed January 10, 2023.
8. LeBrun DG, Shen TS, Bovonratwet P, Morgenstern R, Su EP. Hip resurfacing vs total hip arthroplasty in patients younger than 35 Years: a comparison of revision rates and patient-reported outcomes. *Arthroplast Today*. 2021;11:229–233. https://doi.org/10.1016/j.artd.2021.09.004.
9. Kumar P, Ksheersagar V, Aggarwal S, et al. Complications and mid to long term outcomes for hip resurfacing versus total hip replacement: a systematic review and meta-analysis. *Eur J Orthop Surg Traumatol*. 2022. https://doi.org/10.1007/s00590-022-03361-5.
10. Mont MA, Ragland PS, Etienne G, Seyler TM, Schmalzried TP. Hip resurfacing arthroplasty. *J Am Acad Orthop Surg*. 2006;14(8):454–463. https://doi.org/10.5435/00124635-200608000-00003.
11. van der Straeten C, Smet K de. Comparing hip resurfacing arthroplasty (HRA) and total hip arthroplasty (THA). In: Smet K de, Campbell P, van der Straeten C, eds. *The Hip Resurfacing Handbook: A Practical Guide to the Use and Management of Modern Hip Resurfacings*. Oxford: Woodhead Publishing; 2013:506–520. Woodhead Publishing series in Biomaterials, *2049-9485*; number 47.
12. Amstutz HC, Le Duff MJ. Hip resurfacing: history, current status, and future. *Hip Int*. 2015;25(4):330–338. https://doi.org/10.5301/hipint.5000268.
13. Sershon R, Balkissoon R, Della Valle CJ. Current indications for hip resurfacing arthroplasty in 2016. *Curr Rev Musculoskelet Med*. 2016;9(1):84–92. https://doi.org/10.1007/s12178-016-9324-0.
14. Evans JT, Evans JP, Walker RW, Blom AW, Whitehouse MR, Sayers A. How long does a hip replacement last? A systematic review and meta-analysis of case series and national registry reports with more than 15 years of follow-up. *Lancet*. 2019;393(10172):647–654. https://doi.org/10.1016/S0140-6736(18)31665-9.
15. Merola M, Affatato S. Materials for hip prostheses: a review of wear and loading considerations. *Materials*. 2019;12.
16. Grieco PW, Pascal S, Newman JM, et al. New alternate bearing surfaces in total hip arthroplasty: a review of the current literature. *J Clin Orthop Trauma*. 2018;9(1):7–16. https://doi.org/10.1016/j.jcot.2017.10.013.
17. Scholes SC, Burgess IC, Marsden HR, Unsworth A, Jones E, Smith N. Compliant layer acetabular cups: friction testing of a range of materials and designs for a new generation of prosthesis that mimics the natural joint. *Proc Inst Mech Eng H*. 2006;220(5):583–596. https://doi.org/10.1243/09544119H06404.
18. Pritchett JW. Total articular knee replacement using polyurethane. *J Knee Surg*. 2020;33(3):242–246. https://doi.org/10.1055/s-0039-1677816.
19. Nuss KMR, Rechenberg B von. Biocompatibility issues with modern implants in bone - a review for clinical orthopedics. *Open Orthop J*. 2008;2:66–78. https://doi.org/10.2174/1874325000802010066.
20. Münker TJAG, van de Vijfeijken SECM, Mulder CS, et al. Effects of sterilization on the mechanical properties of poly(methyl methacrylate) based personalized medical devices. *J Mech Behav Biomed Mater*. 2018;81:168–172. https://doi.org/10.1016/j.jmbbm.2018.01.033.
21. Zhao C, Pan F, Zhao S, Pan H, Song K, Tang A. Microstructure, corrosion behavior and cytotoxicity of biodegradable Mg-Sn implant alloys prepared by sub-rapid solidification. *Mater Sci Eng C*. 2015;54:245–251. https://doi.org/10.1016/j.msec.2015.05.042.
22. Liu Q, Li W, Cao L, et al. Response of MG63 osteoblast cells to surface modification of Ti-6Al-4V implant alloy by laser interference lithography. *J Bionic Eng*. 2017;14(3):448–458. https://doi.org/10.1016/S1672-6529(16)60410-9.
23. Tsikandylakis G, Mohaddes M, Cnudde P, Eskelinen A, Kärrholm J, Rolfson O. Head size in primary total hip arthroplasty. *EFORT Open Rev*. 2018;3(5):225–231. https://doi.org/10.1302/2058-5241.3.170061.
24. Affatato S, ed. *Perspectives in Total Hip Arthroplasty: Advances in Biomaterials and Their Tribological Interactions*. first ed. Elsevier; 2014.
25. Aguilar HN, Battié MC, Jaremko JL. MRI-based hip cartilage measures in osteoarthritic and non-osteoarthritic individuals: a systematic review. *RMD Open*. 2017;3(1), e000358. https://doi.org/10.1136/rmdopen-2016-000358.
26. Shepherd DE, Seedhom BB. Thickness of human articular cartilage in joints of the lower limb. *Ann Rheum Dis*. 1999;58(1):27–34. https://doi.org/10.1136/ard.58.1.27.
27. Naish JH, Xanthopoulos E, Hutchinson CE, Waterton JC, Taylor CJ. MR measurement of articular cartilage thickness distribution in the hip. *Osteoarthritis Cartilage*. 2006;14(10):967–973. https://doi.org/10.1016/j.joca.2006.03.017.
28. Fiedler BA, ed. *Managing Medical Devices within a Regulatory Framework*. Elsevier; 2017.
29. O'Brien J, Wilson I, Orton T, Pognan F. Investigation of the Alamar Blue (resazurin) fluorescent dye for the assessment of mammalian cell cytotoxicity. *Eur J Biochem*. 2000;267(17):5421–5426. https://doi.org/10.1046/j.1432-1327.2000.01606.x.
30. Rampersad SN. Multiple applications of Alamar Blue as an indicator of metabolic function and cellular health in cell viability bioassays. *Sensors*. 2012;12(9):12347–12360. https://doi.org/10.3390/s120912347.
31. Barua P, You MP, Bayliss K, Lanoiselet V, Barbetti MJ. A rapid and miniaturized system using Alamar blue to assess fungal spore viability: implications for biosecurity. *Eur J Plant Pathol*. 2017;148(1):139–150. https://doi.org/10.1007/s10658-016-1077-5.
32. Wandiyanto JV, Truong VK, Al Kobaisi M, et al. The fate of osteoblast-like MG-63 cells on pre-infected bactericidal nanostructured titanium surfaces. *Materials*. 2019;12(10). https://doi.org/10.3390/ma12101575.
33. Münker TJAG, van de Vijfeijken SECM, Mulder CS, et al. Effects of sterilization on the mechanical properties of poly(methyl methacrylate) based personalized medical devices. *J Mech Behav Biomed Mater*. 2018;81:168–172. https://doi.org/10.1016/j.jmbbm.2018.01.033.
34. Lucas AD, Merritt K, Hitchins VM, et al. Residual ethylene oxide in medical devices and device material. *J Biomed Mater Res B Appl Biomater*. 2003;66(2):548–552. https://doi.org/10.1002/jbm.b.10036.
35. Basri H, Syahrom A, Prakoso AT, et al. The analysis of dimple geometry on artificial hip joint to the performance of lubrication. *J Phys.: Conf Ser*. 2019;1198(4), 42012. https://doi.org/10.1088/1742-6596/1198/4/042012.
36. Ammarullah M, Santoso G, Sugiharto S, et al. Minimizing risk of failure from ceramic-on-ceramic total hip prosthesis by selecting ceramic materials based on tresca stress. *Sustainability*. 2022;14(20), 13413. https://doi.org/10.3390/su142013413.
37. Kaya M, Suzuki T, Emori M, Yamashita T. Hip morphology influences the pattern of articular cartilage damage. *Knee Surg Sports Traumatol Arthrosc*. 2016;24(6):2016–2023. https://doi.org/10.1007/s00167-014-3297-6.
38. Ammarullah MI, Md Saad AP, Syahrom A, Basri H. Contact pressure analysis of acetabular cup surface with dimple addition on total hip arthroplasty using finite element method. *IOP Conf Ser Mater Sci Eng*. 2021;1034(1), 12001. https://doi.org/10.1088/1757-899X/1034/1/012001.
39. Ruggiero A, Merola M, Affatato S. Finite element simulations of hard-on-soft hip joint prosthesis accounting for dynamic loads calculated from a musculoskeletal model during walking. *Materials*. 2018;11(4). https://doi.org/10.3390/ma11040574.